ARCHIVES OF ELECTRICAL ENGINEERING VOL. 63(4), pp. 551-578 (2014)

DOI 10.2478/aee-2014-0038

# Improvement of microgrid dynamic performance under fault circumstances using ANFIS for fast varying solar radiation and fuzzy logic controller for wind system

MAZIAR IZADBAKHSH, ALIREZA REZVANI, MAJID GANDOMKAR

*Department of Electrical Engineering, Saveh Branch, Islamic Azad University, Saveh, Iran*
*e-mail: m.izadbakhsh@iau-saveh.ac.ir*

(Received: 20.05.2014, revised: 11.08.2014)

**Abstract:** The microgrid (MG) technology integrates distributed generations, energy storage elements and loads. In this paper, dynamic performance enhancement of an MG consisting of wind turbine was investigated using permanent magnet synchronous generation (PMSG), photovoltaic (PV), microturbine generation (MTG) systems and flywheel under different circumstances. In order to maximize the output of solar arrays, maximum power point tracking (MPPT) technique was used by an adaptive neuro-fuzzy inference system (ANFIS); also, control of turbine output power in high speed winds was achieved using pitch angle control technic by fuzzy logic. For tracking the maximum point, the proposed ANFIS was trained by the optimum values. The simulation results showed that the ANFIS controller of grid-connected mode could easily meet the load demand with less fluctuation around the maximum power point. Moreover, pitch angle controller, which was based on fuzzy logic with wind speed and active power as the inputs, could have faster responses, thereby leading to flatter power curves, enhancement of the dynamic performance of wind turbine and prevention of both frazzle and mechanical damages to PMSG. The thorough wind power generation system, PV system, MTG, flywheel and power electronic converter interface were proposed by using Mat-lab/Simulink.

**Key words:** MG, dynamic performance, photovoltaic, PMSG, ANFIS, droop control

## 1. Introduction

Nowadays, the world is looking for energy alternative sources as the energy demand continues to grow. Wind, PV, MTG are three of the most promising renewable power generation technologies due to their advantages. However, each of the aforementioned technologies has its own drawbacks. Interconnection networks of distributed energy resources, energy storage systems and loads define an MG that can operate in stand-alone or in grid-connected mode [1, 2]. An MG is disconnected automatically from the main distribution system and changed to islanded operation when a fault occurs in the main grid or the power quality of the

Brought to you by | Biblioteka Główna Zachodniopomorskiego Uniwersytetu Technologicznego w Szczecinie
Authenticated
Download Date | 3/5/15 11:09 AM

grid falls below a required standard. In the grid connected mode, the grid dominates most of the system dynamics and no significant problem needs to be addressed except the power flow control, whereas in the islanding mode, once the isolating switch disconnected the utility from the MG [3, 4].

Developing PV energy sources can reduce fossil fuel dependency [5]. In recent years, many different technics have been applied in order to reach the maximum power. The most prevalent technics are perturbation and observation (P&O) algorithm [6, 7], Incremental conductance (IC) [8, 9], fuzzy logic [10, 11] and artificial networks (ANN) [12-14]. According to the above mentioned researches, the benefits of perturbation and observation algorithm and incremental conductance are: 1 – low cost implementation, and 2 – simple algorithm. The depletion of these methods is vast fluctuation of output power around the MPP even under steady state, resulting in the loss of available energy [15].

Using fuzzy logic can solve the two mentioned problems dramatically. In fact, with fuzzy logic controller, proper switching can reduce oscillations of output power around the MPP and losses. Furthermore, in this way, convergence speed is higher than the other two ways mentioned. A weakness of fuzzy logic, compared to neural network, refers to oscillations of output power around the MPP [16]. Nowadays, artificial intelligence (AI) techniques have numerous applications in determining the size of PV systems, MPPT control and the optimal structure of photovoltaic systems [17].

Neural networks can be considered as a powerful technique for mapping inputs-outputs of non-linear functions, but it lacks subjective sensations and acts as a black box. On the other hand, through fuzzy rules and membership functions, fuzzy logic has the ability to transform linguistic and mental data into numerical values. However, the determination of membership functions and fuzzy rules depends on the previous knowledge of the system. Neural networks can be integrated with fuzzy logic and through the combination of these two smart tools, a robust AI technique called ANFIS can be obtained [18]. In [19, 20], the structure of ANFIS have been used, but one of the major drawbacks in these articles is that they were not connected to the grid in order to ensure the analysis of system performance, which was not considered.

In terms of wind power generation system (WPGS), it is proposed as one of the outstanding renewable energy sources [21, 22]. One of the approaches used to reach the MPP is pitch angle control, in which small turbines with low power delivery are not possible due to mechanical difficulties in production [23].

In the past, PIDs were used mostly in controllers design, but by the introduction of fuzzy logic instead of PID created a better performance such that it was the best preventative way to eliminate the profound mathematical understanding of system. Comparing PIDs and fuzzy logic systems shows that fuzzy logic has more stability, faster and smoother response, and smaller overshoot. It does not need a fast processor, and is more powerful than other non-linear controllers too [24]. In [25-27], a pitch angle controller based on fuzzy logic was presented. In [27], active power and in [25, 27], both reactive power and rotational rotor speed were used as input signals. As in the mentioned items wind speed was ignored, the controller did not show as fast response and could cause mechanical damages to the synchronous

Brought to you by | Biblioteka Główna Zachodniopomorskiego Uniwersytetu Technologicznego w Szczecinie
Authenticated
Download Date | 3/5/15 11:09 AM

generator. Also, another problem with these studies was that they were not practically connected to grid to analyze the system performance [26-28].

In this paper, the simulation and structure of MTG and flywheel have been presented, as investigated in [29-31].

The system modeling for grid, load and inverter in MG has been discussed in [32]. The authors in [33] studied the MG during both connected and islanding modes. In [34], the researchers described the feasibility of a control strategy adopted in the operation of the MG during the islanding mode.

The MG's grid connected operation during and subsequent to the islanding mode were presented in [35], but the DGs dynamic model was not included, which could have a great effect on the dynamic performances of the MG subsequent to islanding. Furthermore, DGs (wind, PV, MTG and etc.) were not considered in their model. Virtually, in the former references, the grid connected process has not discussed to show the effect of wind speed fluctuations in dynamic performances of the MG, especially after the islanding occurrence. In [36], a very simple structure of an MG with three DGs has been studied; however; there is no mention or analysis of the DGs structure, controllers of each micro source, fault occurrence in the grid and response of MG against the sudden circumstances, and the exchanged power between DGs. In [37, 38], authors utilized perturbation and observation algorithm in a PV and wind system in which the mentioned algorithm had vast fluctuation of output power around the MPP even under the steady state. Furthermore, in mentioned paper, there was not any controller (pitch angle control) to control the output power of wind turbine in high speed as it could cause the damages to generator; also, the P-Q control method for wind system was not used in the grid side inverter.

In this paper, three issues were addressed in order to overcome the disadvantages of the aforementioned references: 1) the use of complete model that described in detail all the MG elements (DGs, converter control schemes, control strategies (P-Q and droop control) and etc), 2) the application of fuzzy controller (for pitch angle) instead of PI controller to smooth the output power of wind turbines caused by wind speed fluctuations and a comparison of the performances of the fuzzy controller with the conventional PI controller, and 3) the application of ANFIS controller to capture the MPPT of photovoltaic panels mounted in the MG. Temperature and irradiance as inputs data were given to genetic algorithm and optimal voltage ($V_{mpp}$) corresponding to the MPP delivery from the PV system; then the optimum values were utilized for training the ANFIS.

## 2. Photovoltaic cell model

Figure 1 shows the equivalent circuit of one PV cell [5]. Characteristics of one solar array are explained in following equations:

$$I_{PV} = I_d + I_{RP} + I, \tag{1}$$

Brought to you by | Biblioteka Główna Zachodniopomorskiego Uniwersytetu Technologicznego w Szczecinie
Authenticated
Download Date | 3/5/15 11:09 AM

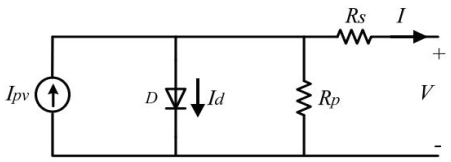


Fig. 1. Equivalent circuit of one PV array

$$I = I_{pv} - I_d\left[\exp\left(\frac{V + R_S I}{V_{th} n}\right) - 1\right] - \frac{V + R_S I}{R_P}, \tag{2}$$

Where $I$ is the output current, $V$ is the output voltage, $I_{pv}$ is the generated current under a given insolation, $I_{RP}$ is diode current, $I_0$ is the diode reverse saturation current, $n$ is the ideality factor for a p-n junction, $R_s$ is the series loss resistance, and $R_p$ is the shunt loss resistance. $V_{th}$ is known as the thermal voltage. Red sun 90w is taken as the reference module for simulation and the name-plate details are given in Table 1. The array is the combination of 4 cells in series and 3 cells in the parallel of the 90w module; hence an array generates 1.1 kW.

Table 1. Red sun 90w

| | |
|---|---|
| $I_{MP}$ (current at maximum power) | 4.94 A |
| $V_{MP}$ (voltage at maximum power) | 18.65 V |
| $P_{MAX}$ (maximum power) | 90 W |
| $V_{OC}$ (open circuit voltage) | 22.32 |
| $I_{SC}$ (short circuit current) | 5.24 |
| $N_P$ (total number of parallel cells) | 1 |
| $N_S$ (total number of series cells) | 36 |

## 3. Maximum power tracking – ANFIS and genetic algorithm technic

### 3.1. The Steps in implementing genetic algorithm

In order to pursue the optimum point for maximum power in any environmental condition, ANFIS and genetic algorithm technic are used. Besides, genetic algorithm is used for optimum values and then optimum values are used for training ANFIS [39, 40]. The procedure employed for implementing genetic algorithm is as follows [41]: 1) defining the objective function and recognizing the design parameters, 2) defining the initial production population, 3) evaluating the population using the objective function, and 4. conducting convergence test stop if convergence is provided.

The objective function of genetic algorithm is used for its optimization (using Matlab software) by the following: finding the optimum $X = (X_1, X_2, X_3,..., X_n)$ to put the $F_{(X)}$ in the maximum value, where the number of design variables are considered as 1. $X$ is the design

Brought to you by | Biblioteka Główna Zachodniopomorskiego Uniwersytetu Technologicznego w Szczecinie
Authenticated
Download Date | 3/5/15 11:09 AM

variable equal to array current and also, $F_{(X)}$ is the array output power which should be maximized [39]. To determine the objective function, the power should be arranged based on the current of array ($I_X$). The genetic algorithm parameters are given in Table 2.

$$F_{(X)} = V_X * I_X, \tag{3}$$

$$0 < I_X < I_{SC}. \tag{4}$$

Table 2. The genetic algorithm parameters

| | |
|---|---|
| Number of design variable | 1 |
| Population size | 20 |
| Crossover constant | 80% |
| Mutation rate | 10% |
| Maximum generations | 20 |

The current constraint should be considered too. With maximizing this function, the optimum values for $V_{mpp}$ and MPP will result in any particular temperature and irradiance intensity.

### 3.2. Adaptive neuro-fuzzy inference systems

ANFIS refers to adaptive neuro-fuzzy inference system. An adaptive neural network has the advantages of learning ability, optimization and balancing. However, a fuzzy logic is a method based on rules constructed by the knowledge of experts [42]. The good performance and effectiveness of fuzzy logic have been approved in nonlinear and complicated systems. ANFIS combines the advantages of using adaptive neural network and fuzzy logic. ANFIS makes use of Sugeno type [19, 20]. For a fuzzy inference system, with 2 inputs and 1 output, a common rule set is obtained with 2 fuzzy if-then rules by the following Equations. The fuzzy rules can typically be as follows:

Rule 1. If x is A1 and y is B1; then

$$f1 = p1x + q1y + r1. \tag{5}$$

Rule 2. If x is A2 and y is B2; then

$$f2 = p2x + q2y + r2. \tag{6}$$

Where x and y are the inputs and f is the output. [$A1$, $A2$, $B1$, $B2$] are called the premise parameters. [$pi$, $qi$, $ri$] are called the consequent parameters, $i$ = 1, 2. The consequent parameters ($p$, $q$, and $r$) of the nth rule contribute through a first order polynomial .These parameters are called result parameters. The ANFIS structure of the above statements is shown in Figure 2.

This structure has five layers. It can be seen that the nodes of the same layer have the same functions. i output node in layer 1 is named as $Q_{1i}$.

Brought to you by | Biblioteka Główna Zachodniopomorskiego Uniwersytetu Technologicznego w Szczecinie
Authenticated
Download Date | 3/5/15 11:09 AM

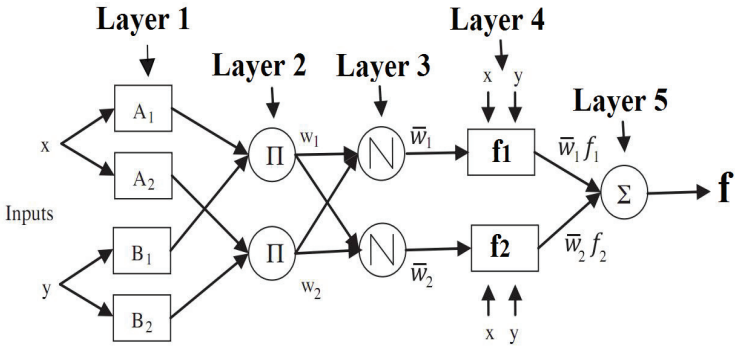


Fig. 2. ANFIS architecture of a 2-input first-order Sugeno fuzzy model with 2 rules

Layer 1. Every node in this layer consists of an adaptive node with a node function. We have:

$$Q_{1,i} = \mu A_i(x), \quad \text{for } i = 1, 2, \tag{7}$$

$$Q_{1,i} = \mu B_{i-2}(y), \quad \text{for } i = 3, 4. \tag{8}$$

Where $x$ (or $y$) is the input of node i and $A_i$ (or $B_i - 2$) is a fuzzy set related to that node. In other words, the output of this layer is its membership value. Membership functions for A can be any appropriate parameterized membership function. Each parameter in this layer is regarded as a default parameter.

Layer 2. Each node in this layer has been labeled with an "$n$" and the output of each node is the product of multiplying all incoming signals for that node. These nodes perform the fuzzy AND operation, and we have:

$$Q_{2,i} = w_i = \mu A_i(x)\mu_{Bi}(y), \quad \textit{for } i = 1, 2, \tag{9}$$

where the output of each node indicates firing strength of each rule.

Layer 3. Each node in this layer has been labeled with an "$N$". Nodes in this layer calculate the normalized output of each rule. Then we have:

$$Q_{3,i} = \overline{w}_i = \frac{W_i}{W_1 + W_2} \quad i = 1, 2, \tag{10}$$

where $W_i$ is the firing strength of that rule. The output of this layer is called the normalized firing strength.

Layer 4. Each node in this layer is associated with a node function. Then we have:

$$Q_{4,i} = \overline{w}_i f_i = \overline{w}_i (p_i x + q_i y + r_i), \tag{11}$$

where $W_i$ is the normalized firing strength of the third layer and $\{p_i, q_i, r_i\}$ are parameters sets of the node $i$. Parameters of this layer are called "consequent parameters".

Brought to you by | Biblioteka Główna Zachodniopomorskiego Uniwersytetu Technologicznego w Szczecinie
Authenticated
Download Date | 3/5/15 11:09 AM

Layer 5. The single existing node in this layer is labeled as Σ. It computes the sum of all its input signals and sends them to the output section.

$$Q_{5,i} = \sum \overline{w}_i f_i = \frac{\Sigma_i w_i f_i}{\Sigma_i \ w_i}, \tag{12}$$

where $Q_{5i}$ is the output of node ($i$) in the fifth layer. For this reason, first, all existing rules will be established in the layer 1.

In this paper, a hybrid learning algorithm was used. The hybrid learning algorithm is a combination of gradient descent and least squares methods. In this simulation, irradiance and temperature were regarded as the input and output was an optimal voltage ($V_{mpp}$) corresponding to the MPP delivery from the PV system. Then, the output voltage of PV module with ANFIS output voltage was deducted to obtain the error signal. Then, through a PI controller, this error signal was given to a pulse width modulation (PWM) block. The block diagram of the proposed MPPT scheme is shown in Figure 3.

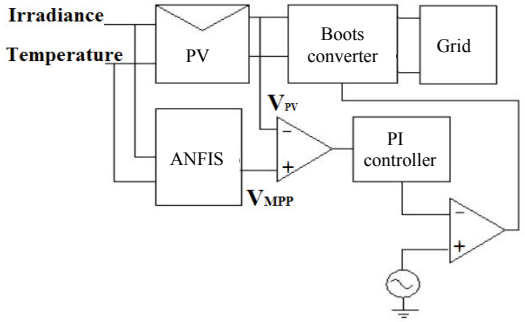


Fig. 3. Proposed MPPT Scheme

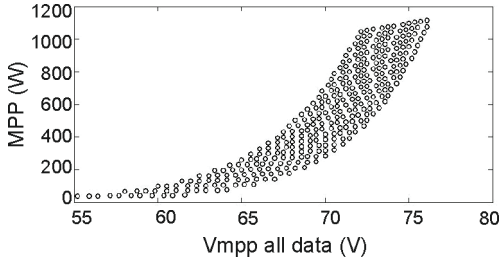


Fig. 4. The output data $V_{mpp}$ corresponding to (MPP)

The PV system was designed in order to obtain data by genetic algorithm. A set of 360 data was put to temperature and irradiance as inputs. Also, the output was $V_{mpp}$ corresponding to the MPP delivery from the PV panels as depicted in Figure 4. Then these optimum values were utilized for training the ANFIS. All input were 360 data in which a set of 330 data was used for training the developed ANFIS model and also, a set of 30 data samples not included in the

Brought to you by | Biblioteka Główna Zachodniopomorskiego Uniwersytetu Technologicznego w Szczecinie
Authenticated
Download Date | 3/5/15 11:09 AM

training was used for the testing. Input temperature ranged from 5 to 55°C in the steps of 5° C and irradiance varied from 50 to 1000 (W/m$^2$) in the steps of 32 (W/m$^2$).

ANFIS input structure is shown in Figure 5. It includes five layers. The two inputs represent irradiance and temperature, both of which have 3 membership functions. The structure shows two inputs of the solar irradiance and cell temperature, which are translated into appropriate membership functions. Three functions for the solar irradiance are shown in Figure 6(a) and three functions for temperature are illustrated in Figure 6(b). The network is trained for 30,000 epochs. After the training process, the output of the trained network should be very close to the target outputs as shown in Figure 7(a). According to Figures 7(b) and 7(c), $V_{mpp}$ was compared with the target value and in Figures 8(a), 8(b) and 8(c) the output of ANFIS test was compared with the target value, showing a negligible training error percentage of about 1.4%.

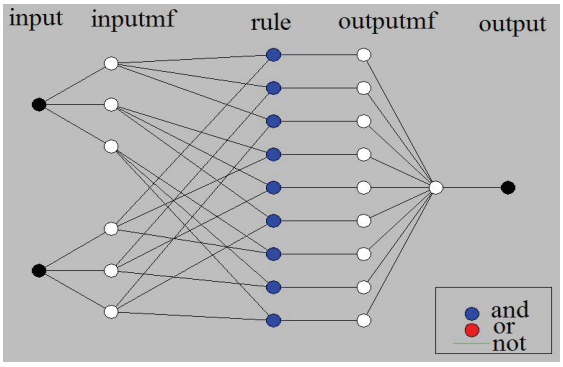


Fig. 5. ANFIS controller structure

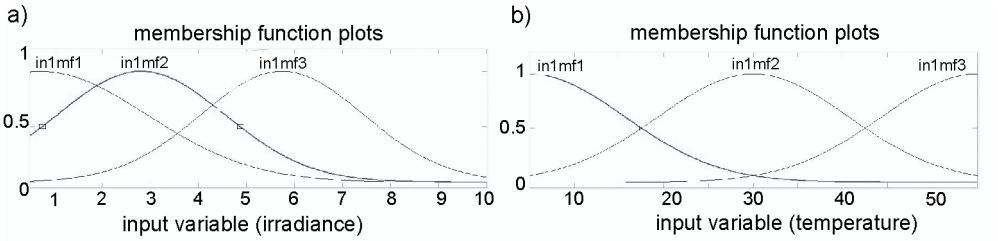


Fig. 6. ANFIS membership function: (a) solar irradiance membership function, (b) temperature membership functions

## 4. Wind system configuration

The diagram of a wind generation system in the presence of PMSG integrated with the grid is illustrated in Figure 9. Turbine output was rectified by using the uncontrolled rectifier. Then dc link voltage was adjusted by PI controller until it reached a constant value and then this constant voltage was inverted to AC voltage using sinusoidal PWM inverter. Inverter adjusted

Brought to you by | Biblioteka Główna Zachodniopomorskiego Uniwersytetu Technologicznego w Szczecinie
Authenticated
Download Date | 3/5/15 11:09 AM

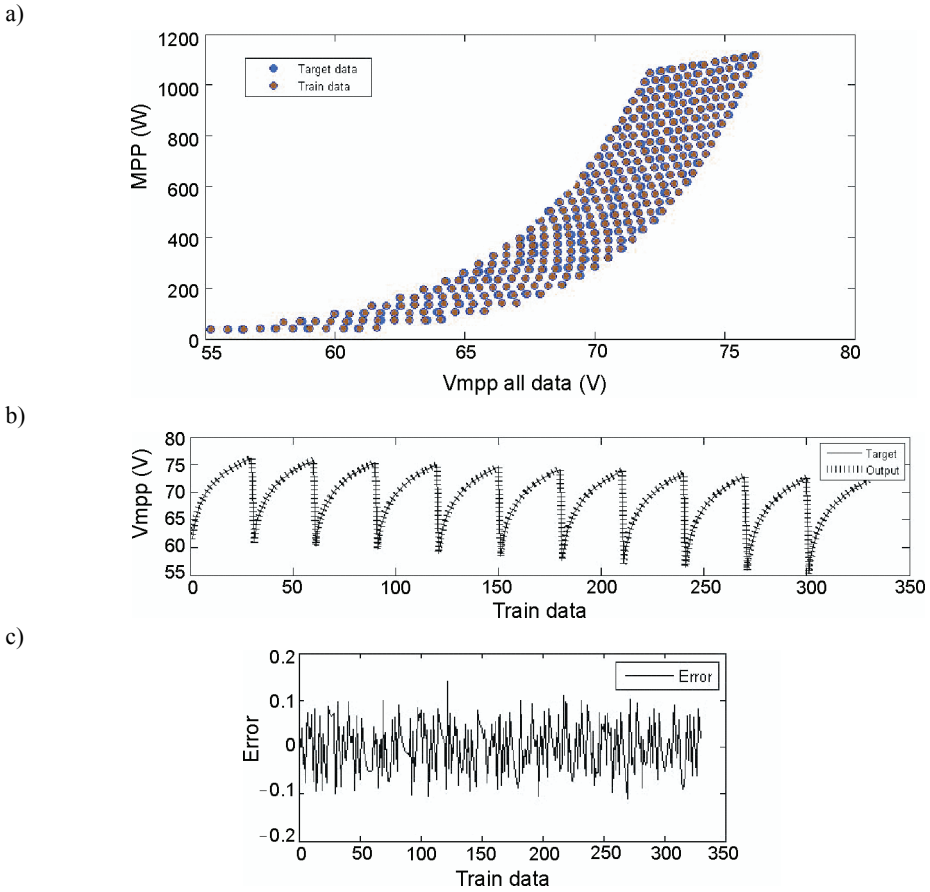


Fig. 7. The output of the ANFIS: (a) The output of the ANFIS with the amount of target data; (b) The output of ANFIS ($V_{mpp}$)with the amount of target data; (c) Percentage error of the ($V_{mpp}$) after training data

the dc link voltage and injected active power by d-axis and injected reactive power by q-axis using P-Q control method. Furthermore, turbine output was regulated through pitch angle controller based on fuzzy logic in extra high wind speeds.

### 4.1. Wind turbine and PMSG modeling

The amount of electricity a turbine is able to produce depends on the speed of the rotor and the speed of the wind that propels the rotor. Aerodynamic wind power is calculated in Equation (13):

$$P = 0.5\,\rho A C_p(\lambda, \beta) V_W^3, \tag{13}$$

Brought to you by | Biblioteka Główna Zachodniopomorskiego Uniwersytetu Technologicznego w Szczecinie
Authenticated
Download Date | 3/5/15 11:09 AM

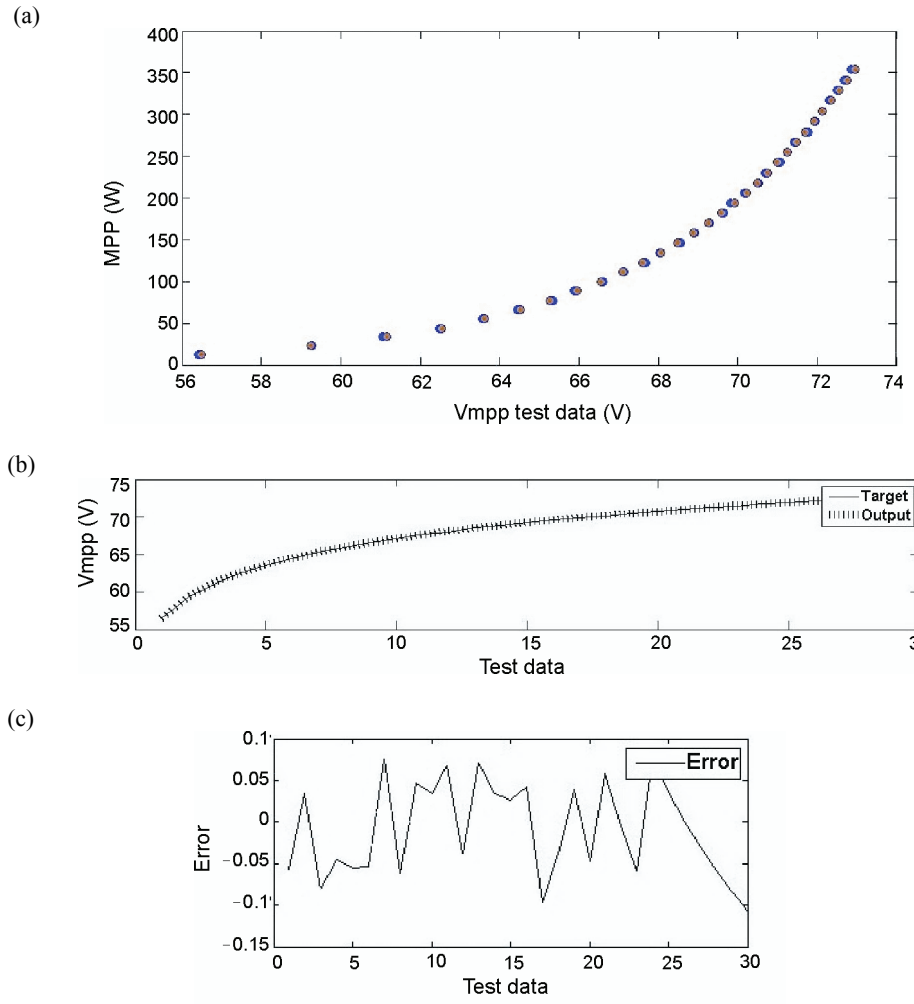


Fig. 8. The output of the ANFIS test: (a) The output of the ANFIS test with the amount of target data; (b) The output of the ANFIS test ($V_{mpp}$) with the amount of target data; (c) Percentage error of test data ($V_{mpp}$) after training data

$$\lambda = \frac{W_m R}{V_w}, \tag{14}$$

where $P$, $\rho$, $A$, $V_w$, $W_m$ and $R$ are power, air density, rotor swept area of the wind turbine, wind speed in m/sec, rotor speed in rad/sec and the radius of the turbine, respectively. Also, $C_P$ is the aerodynamic efficiency of the rotor. PMSG voltage equations and other equations of wind turbine are presented in [28, 43].

Brought to you by | Biblioteka Główna Zachodniopomorskiego Uniwersytetu Technologicznego w Szczecinie
Authenticated
Download Date | 3/5/15 11:09 AM

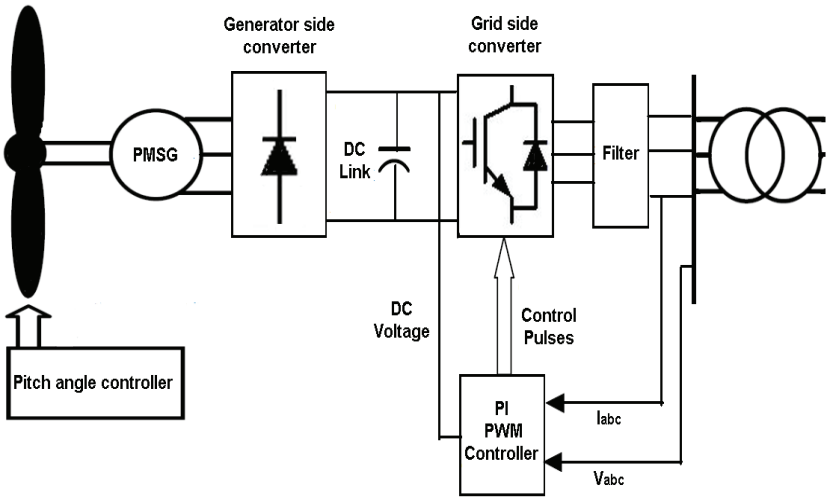


Fig. 9. The block diagram of wind power generation system

### 4.2. Pitch angle based on fuzzy controller

The presented fuzzy controller consists of two input signals and one output signal. The first input signal is based on the deviation between active power and the rated value in P.U, which was mentioned as error signal. Thus, its positive value indicates turbine's normal operation and its negative value shows the extra power generation during the above rated wind speed. In this case, controller should modify pitch angle degree by increasing the nominal value. The pitch angle degree is regulated on zero in a normal condition. The whole wind energy can be converted to mechanical energy and when the pitch angle starts to increase from the zero value, the wind attach angle to the blades will be increased, thereby leading to aerodynamic power reduction and consequently, drawing down the output power. Besides, the second signal is taken from anemometer nacelle [44].

Controller's response is so faster when wind speed is used as an input signal compared to the time when inputs are rotor rotational speed or active power in large turbines with a high moment of inertia [25-27]. However, mechanical erosion in large and high speed turbines will be diminished by adjusting this fuzzy controller. Designing a pitch angle controller based on fuzzy logic for wind turbine power adjustment in high wind speeds is being proposed in this paper. Three Gaussian membership functions are considered in this paper. Also, Min-Max method is used as a defuzzification reference mechanism for Centroid. The membership functions are shown in Figure 10.

Moreover, The rules implemented to obtain the required pitch angle (β) are shown in Table 3.The linguistic variables are represented by VG(very great), SG (small great),OP (optimum), SL (small low),and VL (very low) for error signal and VL (very low), SL (small low), OP (optimum), SH (small high) and VH (very high) for wind speed signal and NL (negative large), NS (negative small), Z (zero), PS (positive small) and PL (positive large) for output signal, respectively.

Brought to you by | Biblioteka Główna Zachodniopomorskiego Uniwersytetu Technologicznego w Szczecinie
Authenticated
Download Date | 3/5/15 11:09 AM

Table 3. Fuzzy rules

| Pitch command | | Active power (error) | | | | |
|---|---|---|---|---|---|---|
| | | VG | SG | OP | SL | VL |
| Wind speed | VL | PL | PS | Z | Z | Z |
| | SL | PL | PS | Z | Z | Z |
| | OP | PL | PS | Z | Z | Z |
| | SH | PL | PS | PS | PS | PS |
| | VH | PL | PL | PL | PL | PL |

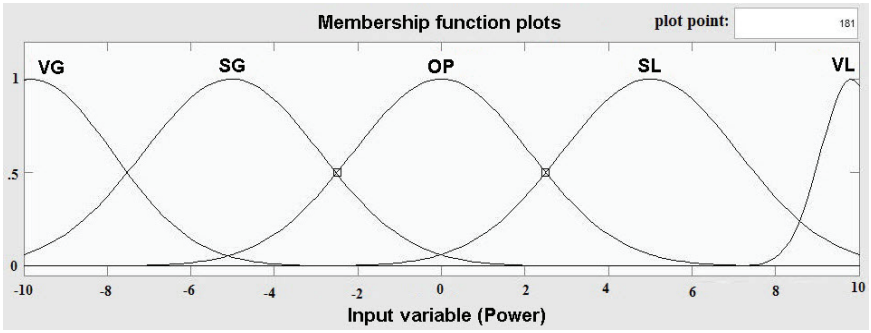


(a)

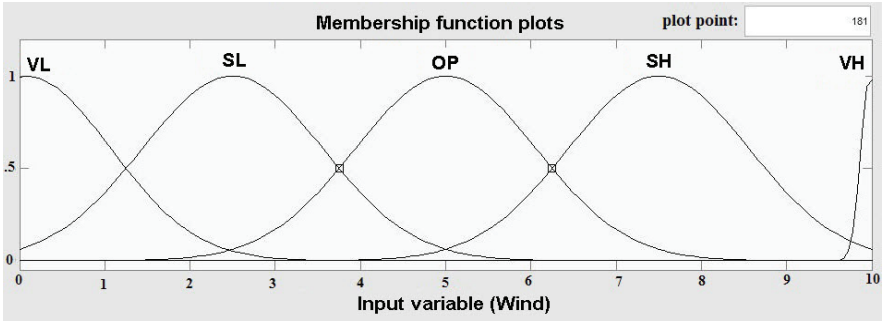


(b)

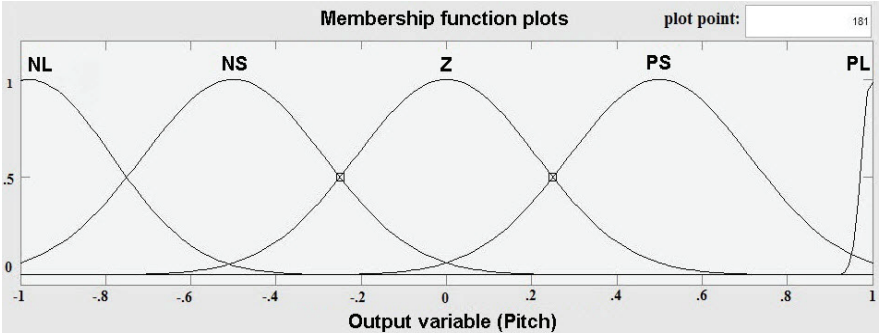


(c)

Fig. 10. The membership function of fuzzy logic: (a) Membership functions of active power (error signal); (b) Membership functions of wind speed; (c) Membership functions of output (β)

Brought to you by | Biblioteka Główna Zachodniopomorskiego Uniwersytetu Technologicznego w Szczecinie
Authenticated
Download Date | 3/5/15 11:09 AM

## 5. MTG system configuration

The modeling and simulation of a single-shift MTG is presented in Figure 11. This model includes the speed governor, acceleration control block, temperature control and fuel system control. MTG details are presented in [29]. The power producer is a synchronous generator with a permanent magnet, which has two poles and a salient pole rotor. The generator produces a high frequency three-phase signal of about 1500 to 4000 Hz. This high frequency voltage is rectified by rectifiers, and then converted to a voltage of 60 Hz by the inverter. The rated output power generated by MTG is 25 kW. The nominal design speed of the generator is 66000 rpm.

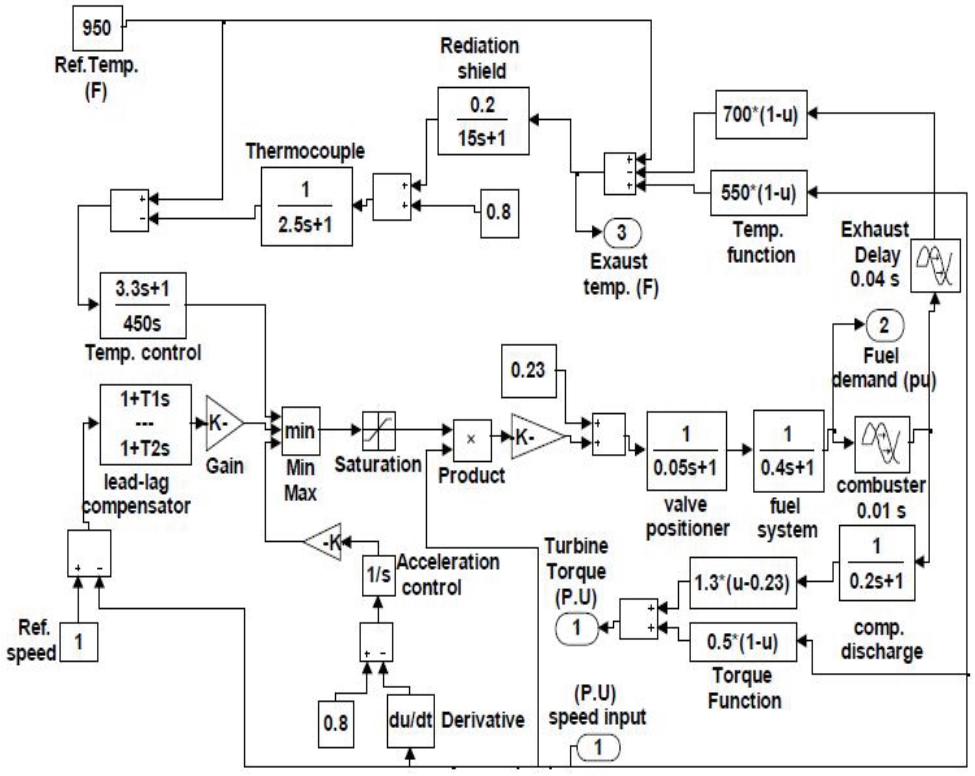


Fig. 11. Simulink implementation of microturbine model

## 6. Flywheel energy storage system (FESS)

As one type of storage device, flywheel has a comparatively fast response. Therefore, flywheel is generally useful when there is an imbalance between supply and demand. In MG, the flywheel can handle the power demands of the peak load and store the energy at the low

Brought to you by | Biblioteka Główna Zachodniopomorskiego Uniwersytetu Technologicznego w Szczecinie
Authenticated
Download Date | 3/5/15 11:09 AM

load period. The flywheel can contribute to the stability of MG voltage amplitude and frequency. Flywheel is connected at the DC bus to provide instantaneous power required by droop controller. In this paper, the storage device used is a flywheel connected to the voltage sources inverter (VSI). The detailed model of flywheel has been presented in [31].

## 7. Control strategies

### 7.1. P-Q control strategy

Inverter control model has been illustrated in Figure 12. The goal of controlling the grid side is keeping the dc link voltage in a constant value regardless of production power magnitude. Internal control-loop controls the grid current and external control loop controls the voltage. Also, internal control-loop is responsible for power quality such as low Total harmonic distortion (THD) and the improvement of power quality and external control-loop is responsible for balancing the power. For reactive power control, reference voltage will be set the same as dc link voltage. In grid-connected mode MG must supply local needs to decrease power from the main grid.

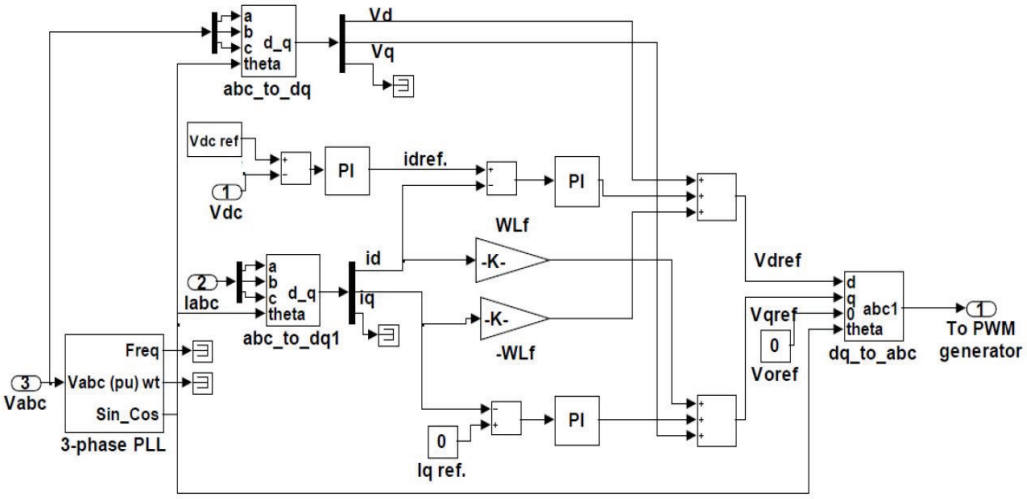


Fig. 12. The P-Q control model

One of the main aspects of P-Q control loop is operating in grid connected and stand-alone mode. The advantages of this operation mode are higher power reliability and higher power quality [45]. Active and reactive components of the injected current are $i_d$ and $i_q$, respectively. $i_q$ current reference is set to zero in order to obtain only a transfer of active power. For the independent control of both $i_d$ and $i_q$, the decoupling terms are used. To synchronize the converter with grid, a three Phase lock loop (PLL) is used.

Brought to you by | Biblioteka Główna Zachodniopomorskiego Uniwersytetu Technologicznego w Szczecinie
Authenticated
Download Date | 3/5/15 11:09 AM

### 7.2. Droop control strategy

The VSI is to be coupled with a storage device (Flywheel) to balance load and generation during islanded operation. Its control is performed using droop concepts [34]. The output power of the VSI is defined from the droop characteristics as shown in Figure 13. During islanded operation, when the unbalance of active power and reactive power occur, the frequency and voltage will fluctuate. As a result, the MG will experience a blackout without any effective controller. If the system is transferred to the islanded mode when importing power from the grid, then the generation needs to increase power to balance power in the islanded mode. The new operating point (B) will be set at a frequency ($f_1$) lower than the nominal value ($f_0$). If the system is transferred to the islanded mode when exporting power to the grid, then the new frequency ($f_2$) will be higher [2, 38]. Also, the reactive power is injected when voltage ($V_1$) falls from the nominal value ($V_0$) and absorbs the reactive power if the voltage ($v_2$) rises above its nominal value.

(a)

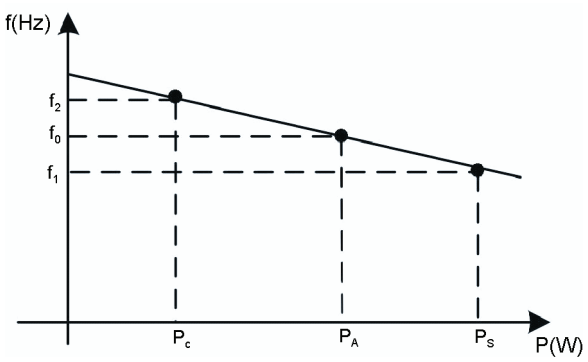


(b)

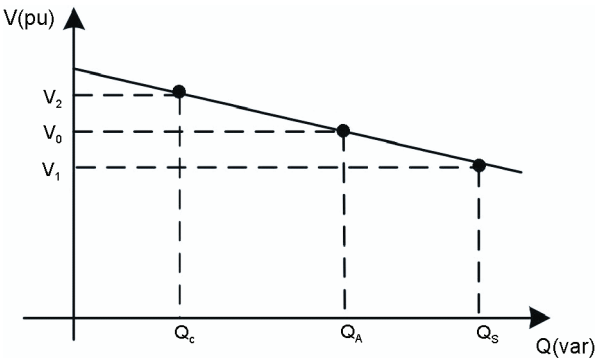


Fig. 13. Droop-characteristics: (a) frequency droop control; (b) voltage droop control

Brought to you by | Biblioteka Główna Zachodniopomorskiego Uniwersytetu Technologicznego w Szczecinie
Authenticated
Download Date | 3/5/15 11:09 AM

### 7.3. Backup controller

Storage devices such as a flywheel have high capabilities for injecting power during islanding operation; however one of the drawbacks is a limited storage capacity. Therefore, it needs the supplementary source to support the frequency deviation. In this case, MTG is utilized for compensating the drifted frequency. The structure of PI controller is illustrated in Figure 14. Restoration of the frequency/voltage of the MG to their normal values requires a supplementary action to adjust the output of the DG [38].

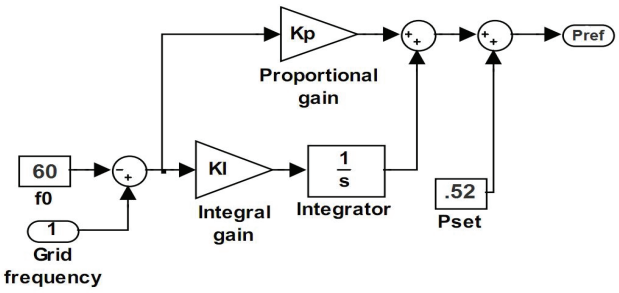


Fig. 14. Back up controller

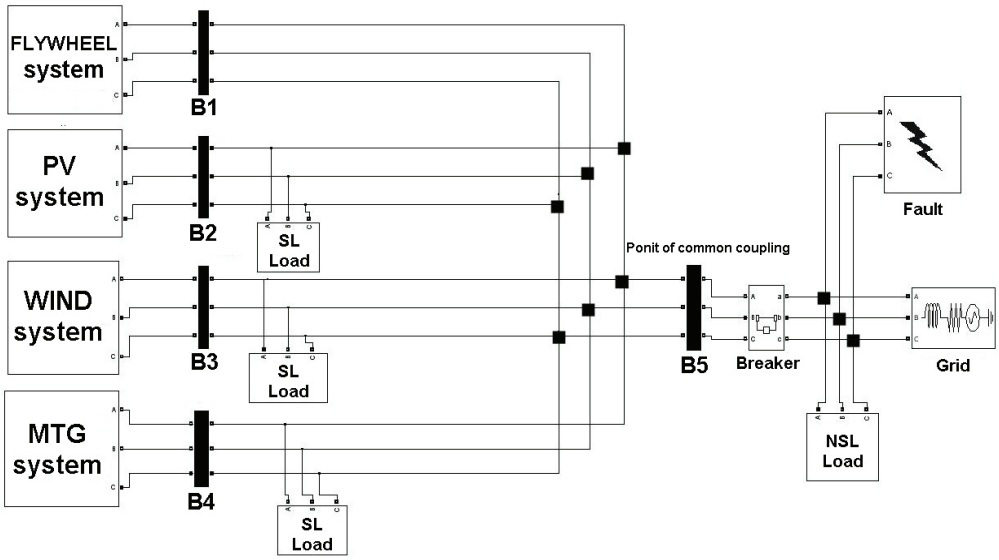


Fig. 15. Case study system

## 8. Simulation results

In this section, simulation results under different terms of operation in MG are presented using Matlab/Simulink. System block diagram is shown in Figure 15. The grid voltage and

Brought to you by | Biblioteka Główna Zachodniopomorskiego Uniwersytetu Technologicznego w Szczecinie
Authenticated
Download Date | 3/5/15 11:09 AM

frequency were 220 V and 60 Hz, respectively. Detailed model descriptions have been given in Appendix A. In Figures 16, 17 and 18, PV, wind system and MTG connected to grid by applying P-Q controller can be seen. Also, Figure 19 shows the FESS connected to grid by applying droop controller.

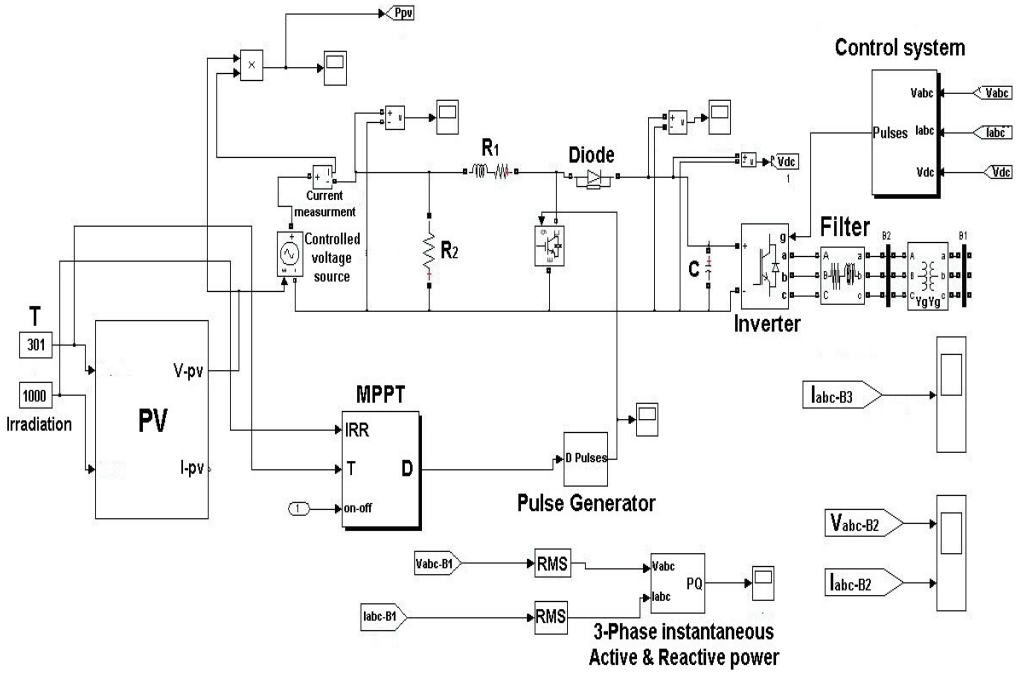


Fig. 16. PV system connected to grid by applying P-Q controller

### 8.1. Case study 1

In this case, the aim was load fault analysis of MG connected to the grid. It was assumed that the sensitive loads (SL) were not connected in MG, and distributed generation sources fed only the non-sensitive load (NSL). The amount of NSL was 75 kW.

The MG included 1.1 kW PV system, 88 kW wind turbine system, 25 kW MTG and 25 kW FESS. The system was controlled by P-Q and droop technic. In the grid connected mode, because storage device (Flywheel) based on droop controller was installed in MG, there was no power exchange between MG and the flywheel. The simulation results for PV are shown in Figure 20. Different irradiance levels, according to Figure 20(a) evaluate the PV's performance. The output current of PV is depicted in Figures 20(b). When irradiance was increased at $t = 2.5$ and $t = 4.5$, it led to the increase in the output current of PV as shown in Figure 20(b). The performance of the proposed controller was compared and analyzed with the conventional techniques of fuzzy logic, P&O and IC. The proposed MPPT algorithm could be converged to MPP's target very fast to track it without any oscillation as shown in Fig. 20(c).

Brought to you by | Biblioteka Główna Zachodniopomorskiego Uniwersytetu Technologicznego w Szczecinie
Authenticated
Download Date | 3/5/15 11:09 AM

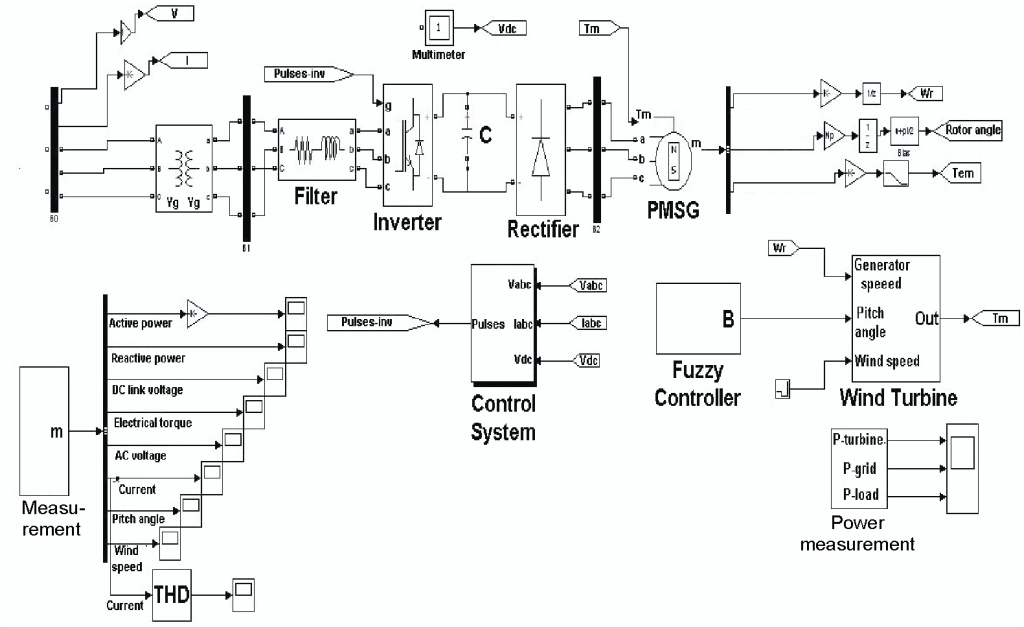


Fig. 17. Wind system connected to grid by applying P-Q controller

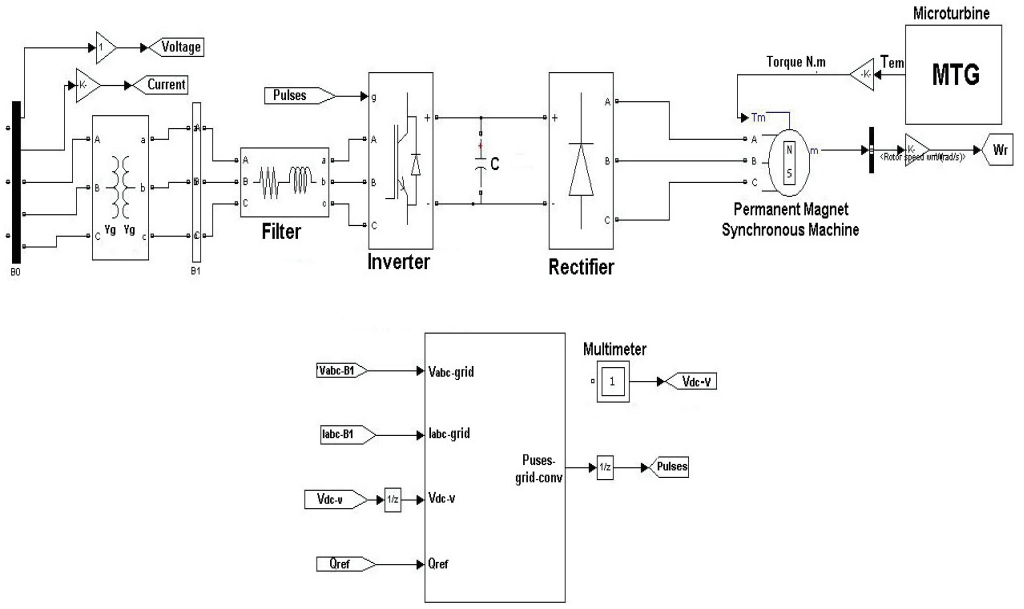


Fig. 18. MTG system connected to grid by applying P-Q and backup controller

Also, in this case, during $0 < t < 1$ sec, the load power was 75 kW and at $t = 1$, it had 40% step increase in load. Wind speed during $0< t <1$ was 11 m/s and at $t = 2.3$ s, it was reduced to 9 m/s. Then, during $1 < t < 2.3$, wind speed was 9 m/s and after that, at $t = 3.8$ s, it was

Brought to you by | Biblioteka Główna Zachodniopomorskiego Uniwersytetu Technologicznego w Szczecinie
Authenticated
Download Date | 3/5/15 11:09 AM

extremely increased to 16m/s. Through designing fuzzy controllers, when wind speed was more than nominal (12 m/s), turbine output power was increased by extremely increasing wind speed; however, without controller, the power was constant at a high level and in the presence of fuzzy controller, it was reduced to the nominal power and made smoother, thereby leading to the prevention of mechanical fatigue to generator.

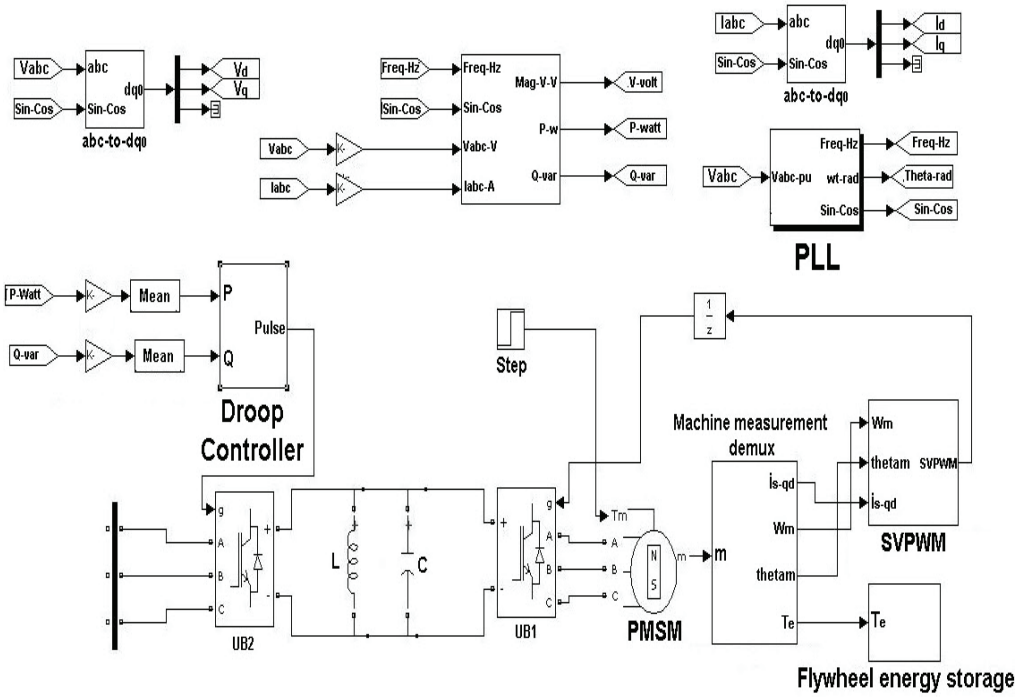


Fig. 19. Flywheel system connected to grid by applying droop controller

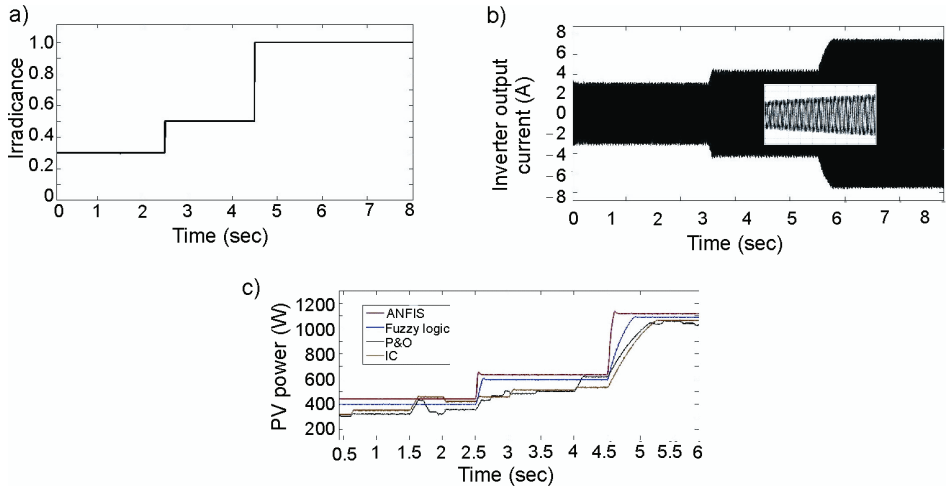


Fig. 20. Simulated results for PV in case 1: a) irradiance ; b) output current of PV (after filter) ; c) PV power

Brought to you by | Biblioteka Główna Zachodniopomorskiego Uniwersytetu Technologicznego w Szczecinie
Authenticated
Download Date | 3/5/15 11:09 AM

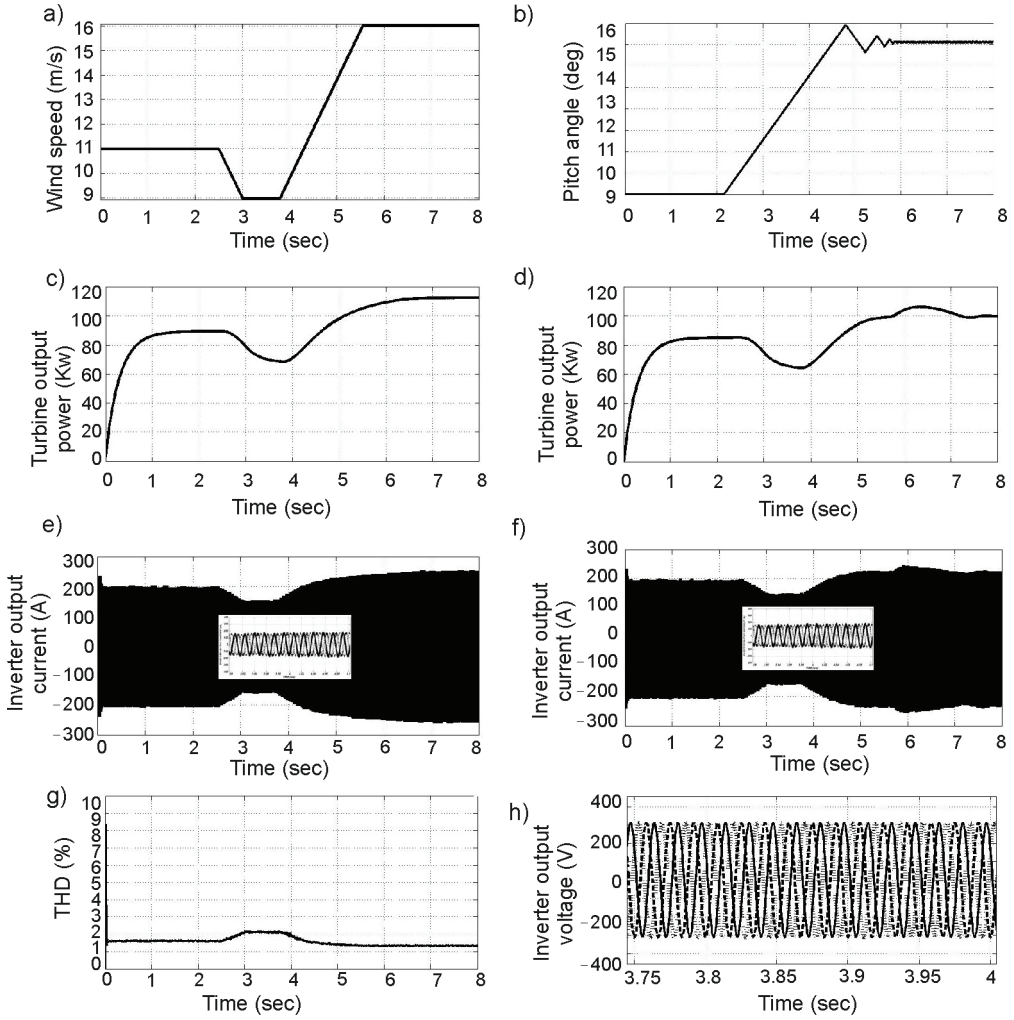


Fig. 21. Simulated results for wind system in case 1: (a) wind speed; (b) variation of pitch angle with presence of fuzzy controller; (c) turbine output power with absence of controller; (d) turbine output power with presence of fuzzy controller; (e) inverter output current with absence of controller; (f) inverter output current with presence of controller; (g) THD(%); (h) Inverter output voltage

Figure 21(a) shows the wind speed used. Figure 21(b) also displays the variation of pitch angle in the presence of controller. As can be seen, in normal situations, the pitch angle was set as zero. At wind speeds above the rated wind, the extracted wind power had to be limited by increasing the pitch angle ($\beta$). Figures 21(c) and 21(d) show the active power of wind turbine in the absence and presence of fuzzy logic controller according to wind speed. It was obvious that fuzzy controller made a smoother power curve. By increasing the pitch angle via fuzzy controller, the exceeding power of wind turbine was limited, reaching to the nominal

Brought to you by | Biblioteka Główna Zachodniopomorskiego Uniwersytetu Technologicznego w Szczecinie
Authenticated
Download Date | 3/5/15 11:09 AM

value. Figures 21(e) and 21(f) show inverter output current in the absence of controller and in the presence of controller, respectively. It shows the effectiveness of fuzzy controller by increasing pitch angle. The exceeding power of wind turbine was limited and also, the inverter output current was reduced in comparison to that without controller.

One of the most important aspects of using DG sources and connecting them to grid is keeping the THD at the minimum of its value. According to IEEE Std.1547.2003, it should be around 5%. In THD curve, it was around 1.5% to 2.5%. THD is shown Figure 21(g). Inverter output voltage, as shown in Figures 21(h), was constant. Figures 22(a) and 22(b) show the grid current in the absence and presence of controller, respectively. It can be observed from Figures 22(c) and 22(d) that pitch angle based on fuzzy controller can limit the exceeding output power of turbine. Therefore, by the reduction of injected output power of wind turbine, the injection of extra total active power of MG to grid was decreased. It is clear that the grid, with the cooperation of wind, PV, MTG systems and FESS, can easily meet the load demand.

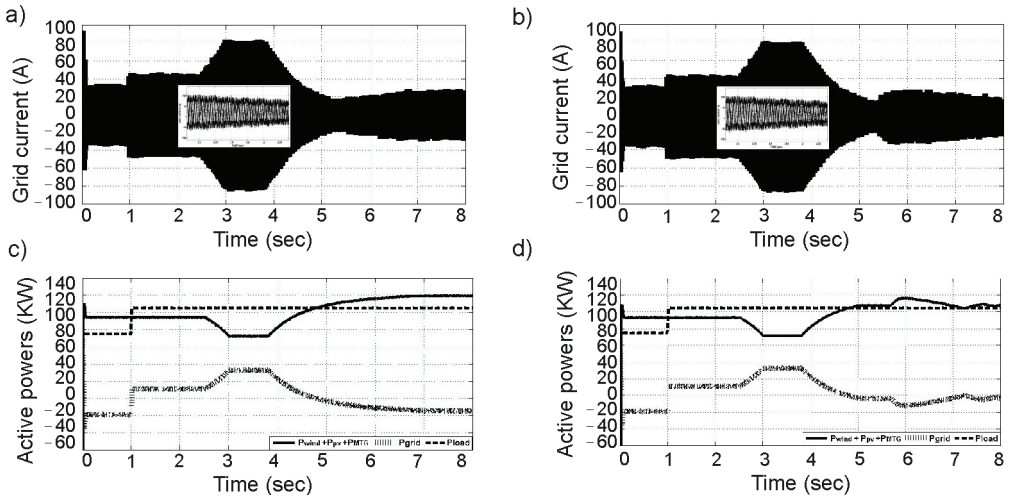


Fig. 22. Simulated results for grid in case 1: (a) Grid current with absence of fuzzy controller; (b) Grid current with presence of fuzzy controller; (c) Active powers with absence of fuzzy controller; (d) Active powers with presence of fuzzy controller

### 8.2. Case study 2

This section aimed to examine the MG from grid connected state to the islanding mode. The MG, after applying a three-phase fault, was separated from the grid. It was assumed that NSL was not connected in MG and the distributed generation sources fed only SL. The MG imported around 15 kW and 11 kvar from the upstream MV network, with a local generation of 93 kW and 5 kvar and an MG load of 108 kW and 16 kvar. Active and reactive power demands in MG are illustrated in Figure 23. Flywheel provided a primary voltage and frequency regulation in the islanded MG. Depending on the load, the (VSI) real and reactive power was defined. The VSI was used to interface the flywheel (storage device) to the MG during and subsequent to the islanding occurrence.

Brought to you by | Biblioteka Główna Zachodniopomorskiego Uniwersytetu Technologicznego w Szczecinie
Authenticated
Download Date | 3/5/15 11:09 AM

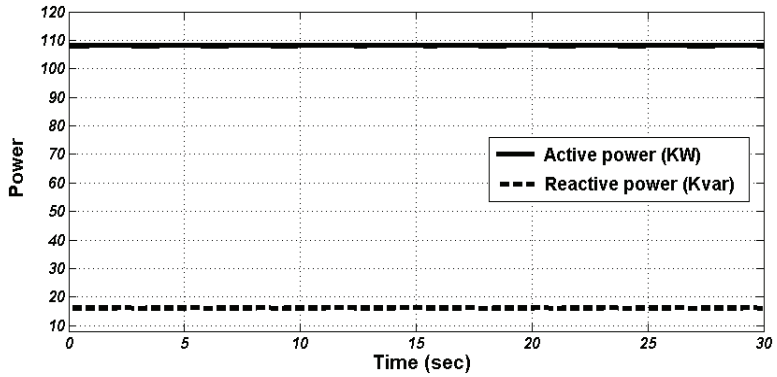


Fig. 23. Active and reactive power demands in MG

At $t$ = 5 sec, the fault was applied to the system and MG became the islanding mode. Also wind power had high fluctuation, leading to high fluctuations in frequency, active and reactive power injected by the VSI, and the voltages of the MG buses. In other words, fuzzy controller acted when wind speed became more than the nominal value. The variation of pitch angle, based on the fuzzy logic in wind turbine, led to smooth turbine output power as shown in Figure 24(a) and 24(b), respectively. Smoothing the output power of wind system led to smooth active power, reactive power, frequency and voltages at all buses of the MG, especially the wind generation bus. During the islanding mode, the reactive power imported from the main grid was lost, and the voltage was dropped to 96% at the bus of wind generation as depicted in Figure 24(c). Then the VSI injected the reactive power to balance the reactive power in the MG as illustrated in Figure 25(a). Frequency deviation forced the VSI to inject the active power according to frequency droop and to balance the generations and loads in the MG, as shown in Figure 25(b). The proposed fuzzy pitch angle controller led to smooth the output power of wind turbine and reduce frequency fluctuations as shown in Figure 26.

The output power of flywheel and MTG in the fuzzy controller had a larger value and less oscillation than PI controller because the fuzzy controller increased the pitch angles of wind turbine, which, in turn, smoothed the output power as shown in Figures 25(b) and 27(a).

The performance of the ANFIS controller in PV was compared and analyzed with the conventional techniques such as fuzzy logic, P&O and IC when operating during a cloudy day with rapid irradiance changes. According to Figure 27(b), it had a good performance and low oscillation in comparison with the mentioned technique. The output power of PV was the same in both cases because PV panel power depended only on irradiance and temperature.

## 9. Conclusion

The presented study was a kind of modeling and analysis of an MG consisting of PMSG wind turbine, PV, MTG systems and FESS under fault circumstances. Variation of wind speed and irradiance and also, the enhancement of dynamic performance of MG were considered.

Brought to you by | Biblioteka Główna Zachodniopomorskiego Uniwersytetu Technologicznego w Szczecinie
Authenticated
Download Date | 3/5/15 11:09 AM

a)

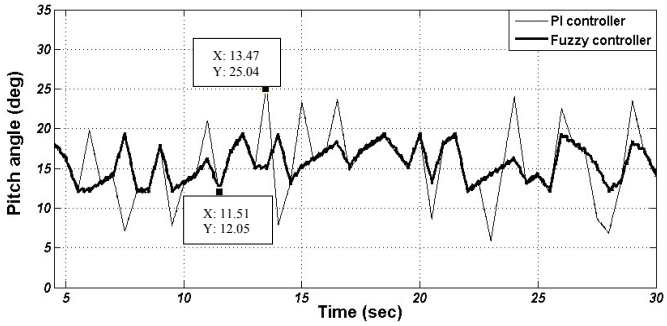


b)

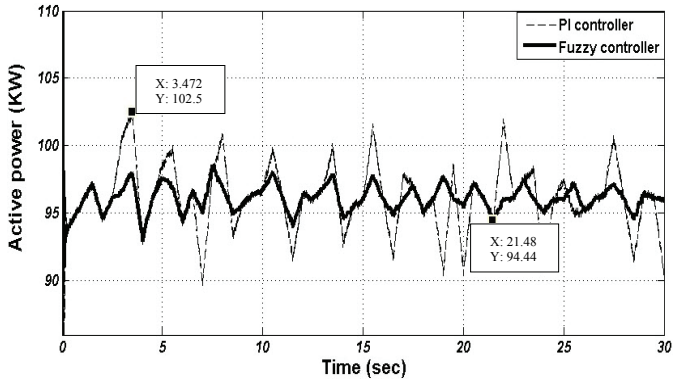


c)

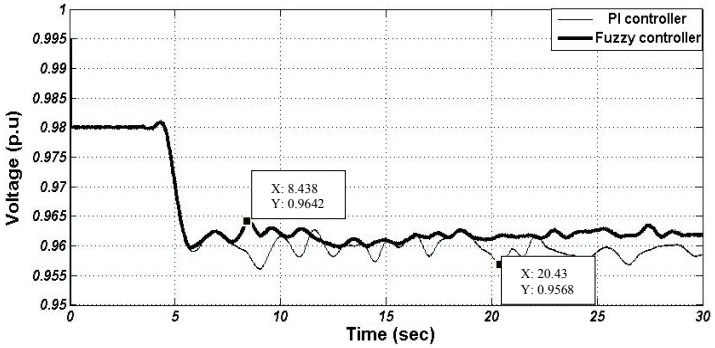


Fig. 24. Wind system: (a) pitch angle (deg); (b) active power; (c) voltage at terminal (bus 3)

The simulation results in the grid connected mode showed that using ANFIS controller could dramatically reduce the disadvantages of the previous approaches. In fact, this research suggested that using ANFIS controller could decrease oscillations of power output around the MPP and increase the convergence speed to achieve the MPP. Also, the presented controller in the wind system, by adding wind speed as an input signal of fuzzy logic, could have a faster and smoother response. The benefit of fuzzy controller is that it keeps the turbine output in an

Brought to you by | Biblioteka Główna Zachodniopomorskiego Uniwersytetu Technologicznego w Szczecinie
Authenticated
Download Date | 3/5/15 11:09 AM

admissible value and can prevent more mechanical erosion and fatigue and also, the dynamic performance of PMSG can be improved. On the other hand, by increasing pitch angle via fuzzy controller, the exceeding power of wind turbine is limited, reaching to the nominal value and reducing inverter output current. Therefore, by the reduction of injected output power of wind turbine, the injection of extra total active power of MG to grid is decreased.

a)

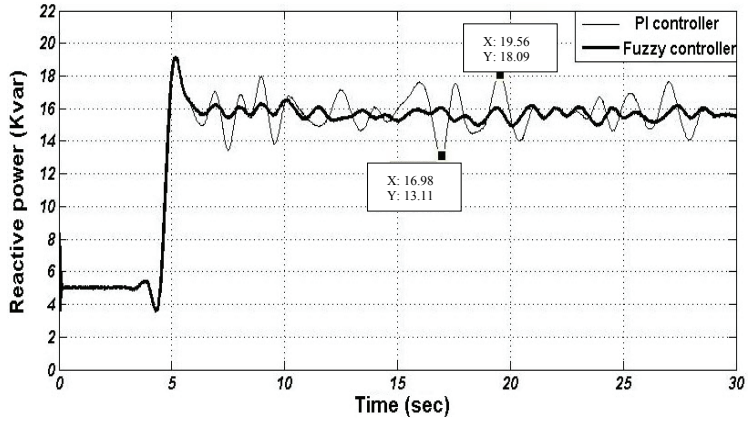


b)

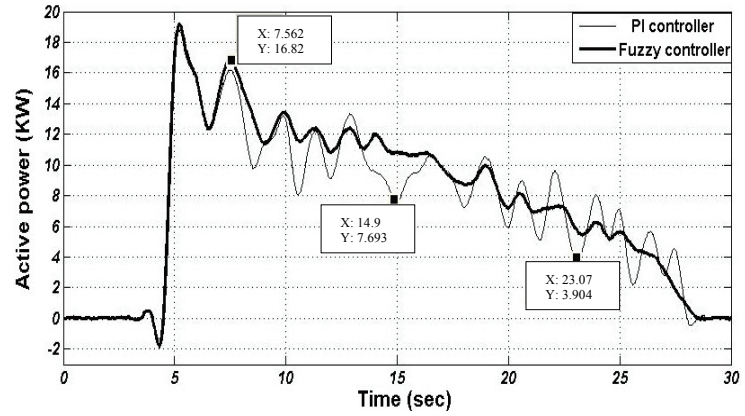


Fig. 25. Flywheel: (a) reactive power; (b) active power

During islanding mode, the performance of the ANFIS controller in PV was compared and analyzed with conventional techniques operating during a cloudy day with rapid irradiance changes, showing that this controller could increase convergence speed to achieve the MPP. Due to the proposed fuzzy controller, it was possible to smooth wind power fluctuations well. Smoothing wind power inside the MG improved the dynamic response of the MG subsequent to the islanding occurrence. The output power of the MTG in the fuzzy controller had a larger value with less oscillation than PI controller because the fuzzy controller increased the pitch angles of wind turbines, which smoothed the output power. Flywheel provided a primary

Brought to you by | Biblioteka Główna Zachodniopomorskiego Uniwersytetu Technologicznego w Szczecinie
Authenticated
Download Date | 3/5/15 11:09 AM

voltage and frequency regulation in the islanded MG. By applying the appropriate controller, the MG in grid-connected mode and islanding mode could meet the load demand assuredly.

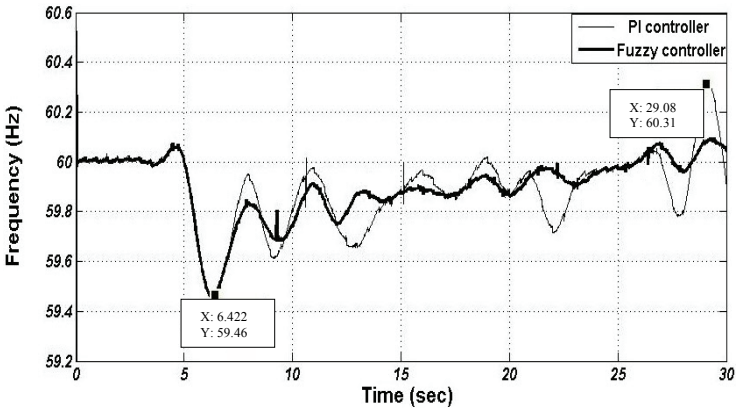


Fig. 26. Frequency variation

a)

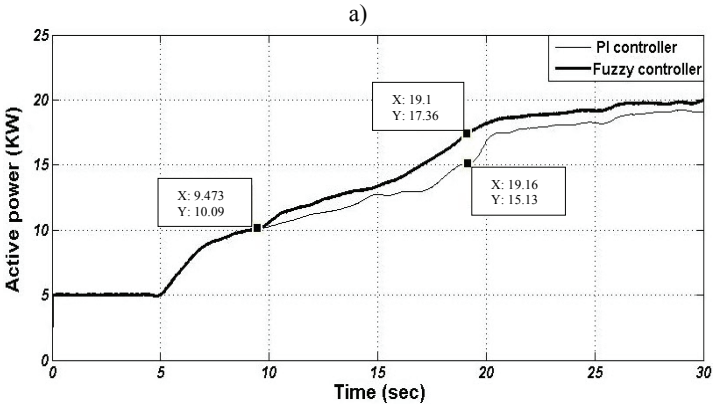


b)

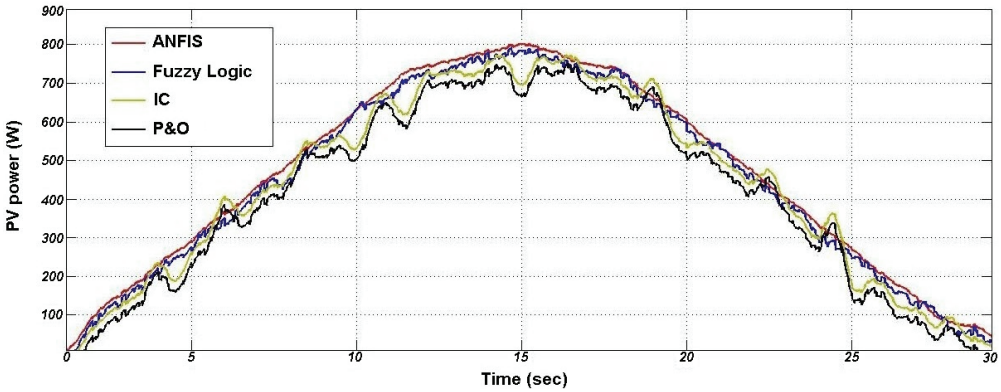


Fig. 27. Generated active power: (a) MTG; (b) PV system

Brought to you by | Biblioteka Główna Zachodniopomorskiego Uniwersytetu Technologicznego w Szczecinie
Authenticated
Download Date | 3/5/15 11:09 AM

**Appendix A. Description of the detailed model**

PV parameters: output power = 1.1 kW, Carrier frequency in $V_{MPPT}$ PWM generator = 4 kHz and in grid-Sid controller = 5.5 kHz, boost converter parameters: $L$ = 5mH, $C$ = 800μF, PI coefficients in grid-side controller: $K_{pVdc}$ = 2, $K_{iVdc}$ = 9, $K_{pId}$ = 10, $K_{iId}$ = 400, $K_{pIq}$ = 10, $K_{iIq}$ = 400.

PMSG parameters: output power = 88 kW, Stator resistance per phase = 2.7 Ω, inertia: 0.9e$^{-3}$ kg-m2, torque constant 12N-M/A, Pole pairs = 8, Nominal speed = 12 m/s, $L_d = L_a$ = 8.9 mH. Grid parameters: X/R = 7, and other parameters, DC link Capacitor = 5300 μF, DC link voltage = 1050. PI coefficients in grid-side controller: $K_{pVdc}$ = 8, $K_{iVdc}$ = 400, $K_{pId}$ = 0.83, $K_{iId}$ = 5, $K_{pIq}$ = 0.83, $K_{iIq}$ = 5.

MTG parameters: MTG ratings = 25 kW, Rotor speed = 66000 rpm, $T_1$ = 0.4, $T_2$ = 1, $K$ = 25. FESS parameters: output power = 25 kW, $J$ = 0.07 Kg.m$^2$, $L$ = 8 mH.

## References

[1] Strauss P., Engler A., *AC coupled PV hybrid systems and MGs-state of the art and future trends.* Proceedings, IEEE 3rd World Conference on Photovoltaic Energy Conversion, Osaka, Japan, pp. 2129-2134 (2003).

[2] Gao D., Jiang J., Qiao S.H., *Comparing the use of two kinds of droop control under microgrid islanded operation mode.* Archives of Electrical Engineering 62(2): 321-331 (2013).

[3] Lasseter R.H., Piagi P., *MicroGrid: a conceptual solution*. Power Electronics Specialists Conference, IEEE 35th Annual, Aachen, Germany; 6: 4285-4290 (2004).

[4] Xiao Zh., Wu J., Jenkins N., *An Overview Of Microgrid Control.* Intelligent Automation & Soft Computing 16: 199-212 (2010).

[5] Hayrettin C., *Model of a photovoltaic panel emulator in MATLAB-Simulink.* Turk. J. Elec. Eng. & Comp. Sci. 21: 301-308 (2013).

[6] Salas V., Olias E., Barrado A., Lazaro A., *Review of the maximum power point tracking algorithms for stand-alone photovoltaic systems*, Solar Energy Materials and Solar Cells 90: 1555-1578 (2006).

[7] Villalva M.G., Gazoli J.R., Filho E., *Comprehensive Approach to Modeling and Simulation of Photovoltaic Arrays.* Power Electronics IEEE Transactions on 24: 1198-1208 (2009).

[8] Chu C.C., Chen C.L., *Robust maximum power point tracking method for photovoltaic cells: a sliding mode control approach.* Solar Energy 83: 1370-1378 (2009).

[9] Liu FF., Duan S., Liu B., Kang Y.A., *Variable step size INC MPPT method for PV systems.* IEEE Trans. Industrial Electronics 55: 622-2628 (2008).

[10] Altin N., *Type-2 Fuzzy Logic Controller Based Maximum Power Point Tracking in Photovoltaic Systems.* Advances in Electrical and Computer Engineering 13: 65-70 (2013).

[11] Gasbaoui B., Abdelkader C.H., Adellah L., *Multi-input multi-output fuzzy logic controller for utility electric vehicle.* Archives of Electrical Engineering 60: 239-256 (2011).

[12] Veerachary M., Senjyu T., Uezato K., *Neural-network-based maximum-power-point tracking of coupled inductor interleaved-boost-converter-supplied PV system using fuzzy controller.* IEEE Transactions on Industria lElectronics 50: 749-758 (2003).

[13] Rai A., K, Kaushika N.D., Singh B., Agarwal N., *Simulation model of ANN based maximum power point tracking controller for solar PV system.* Solar Energy Materials and Solar Cells 95: 773-778 (2011).

[14] Cernazanu C., *Training Neural Networks Using Input Data Characteristics.* Advances in Electrical and Computer Engineering 8: 65-70 (2008).

[15] Esram T, Chapman P.L., *Comparison of photovoltaic array maximum power point tracking techniques*. IEEE Transactions on Energy Conversion 22(2): 439-449 (2007).

[16] Lee S., Kim J., Cha H., *Design and Implementation of Photovoltaic Power Conditioning System using a Current-based Maximum Power Point Tracking.* Journal of Electrical Engineering & Technology 5: 606-613 (2010).

Brought to you by | Biblioteka Główna Zachodniopomorskiego Uniwersytetu Technologicznego w Szczecinie
Authenticated
Download Date | 3/5/15 11:09 AM

[17] Hiyama T., Kitabayashi K., *Neural Network Based Estimation of Maximum Power Generation from PV Module Using Environment Information*, IEEE Transaction on Energy Conversion 12: 241-247 (1997).
[18] Aldobhani A.M.S., John R., *Maximum power point tracking of PV system using ANFIS prediction and fuzzy logic tracking*. IEEE Proceedings of the international multi conference of engineer is and computer scientists IMECS, Hong Kong, pp. 19-21 (2008).
[19] Abu-Ruba H., Iqbalbc A., Ahmeda Sk. M., *Adaptive neuro-fuzzy inference system-based maximum power point tracking of solar PV modules for fast varying solar radiations*, International Journal of Sustainable Energy 31: 383-398 (2012).
[20] Afghoul H., Krim F., Chikouche S., *Increase the photovoltaic conversion efficiency using Neuro-fuzzy control applied to MPPT.* IEEE Renewable and Sustainable Energy Conference IRSEC, Ouarzazate, pp. 348-353 (2013).
[21] Hayatdavudi M., Saeedimoghadam M., Nabavi M.H., *Adaptive Control of Pitch Angle of Wind Turbine using a Novel Strategy for Management of Mechanical Energy Generated by Turbine in Different Wind Velocities.* Journal of Electrical Engineering & Technology 8: 863-871 (2013).
[22] Pourfar I.,Shayanfar H.A., Shanechi H.M., Naghshbandy A.H., *Controlling PMSG-based wind generation by a locally available signal to damp power system inter-area oscillations.* International Transactions On Electrical Energy Systems 23: 1156-1171 (2013).
[23] Yuan Lo K., Chen Y., Chang Y., *MPPT Battery Charger for Stand-Alone Wind Power System*, IEEE Transactions on Power Electronics 26:1631-1638 (2011).
[24] Gaurav N., Kaur A., *Performance Evaluation of Fuzzy Logic and PID Controller by Using MATLAB/Simulink*, International Journal of Innovative Technology and Exploring Engineering (IJITEE) 1: 84-88 (2012).
[25] Lingfeng X., Xiyun Y., Xinran L., Daping X., *Based on adaptive fuzzy sliding mode controller.* IEEE in Intelligent Control and Automation WCICA 7th World Congress on China, Chongqing, pp. 2970-2975 (2008).
[26] Amendola C.A.M., Gonzaga D.P., *Fuzzy-Logic Control System of a Variable-Speed Variable-Pitch Wind-Turbine and a Double-Fed Induction Generator.* IEEE Intelligent Systems Design and Applications, Seventh International Conference, Brazil, pp. 252-257 (2007).
[27] Senjyu T., Sakamoto R., Urasaki N., Funabashi T., Sekine H., *Output power leveling of wind farm using pitch angle control with fuzzy neural network*. IEEE Power Engineering Society General Meeting, Japan, pp. 1-8 (2006).
[28] Yao X., Guo Ch., Xing Z., Li Y., Liu Sh., *Variable Speed Wind Turbine Maximum Power Extraction Based on Fuzzy Logic Control.* IEEE International Conference on Intelligent Human-Machine Systems and Cybernetics, China, pp. 202-205 (2009).
[29] Gaonkar D.N., Patel R.N., Pillai G.N., *Dynamic Model of MTG Generation System for Grid-connected/Islanding Operation.* IEEE International Conference, India, pp. 305-310 (2006).
[30] Qi H.Y., Yi F.B., Feng S.J., *Simulation research on the microgrid with flywheel energy storage system.* Power System Protection and Control 39: 83-87 (2011).
[31] Li W., Yun-li ZH., Wei-dong L., *Simulation System of Flywheel Energy Storage.* Power System and Clean Energy 26: 102-106 (2010).
[32] Zhaoxia X., Chengshan W., Shouxiang W., *Small-signal Stability Analysis of MG Containing Multiple Micro Sources.* Automation of Electric Power Systems 33: 81-85 (2009).
[33] Kanellos F., Tsouchnikas A.I., Hatziargyriou N.D., *Micro-grid simulation during grid-connected and islanded modes of operation.* IPST Presented at the Int. Conf. Power Systems Transients (IPST), Montreal, Canada, IPST, pp. 105-113 (2005).
[34] Lopes J., Moreira C.L., Madureira A.G., *Defining control strategies for micro grids islanded operation*, IEEE Trans. Power Syst. 21: 916-924 (2006).
[35] Katiraei F., Irvani M., Lehn P., *Micro-grid autonomous operation during and subsequent to islanding process*, IEEE Trans. Power Del. 20: 248-257 (2005).
[36] Zamora R., Srivastava A.K., *Controls for Micro-grids with Storage*: *Review, Challenges, and Research Needs.* Elsevier 14: 2009-2018 (2010).

Brought to you by | Biblioteka Główna Zachodniopomorskiego Uniwersytetu Technologicznego w Szczecinie
Authenticated
Download Date | 3/5/15 11:09 AM

[37] Moradian M., Tabatabaei F.M., Moradian S., *Modeling, Control & Fault Management of MGs.* Smart Grid and Renewable Energy 4: 99-112 (2013).
[38] Kamel R.M., Chaouachi A., Nagasaka K., *Detailed Analysis of Micro-Grid Stability during Islanding Mode under Different Load Conditions*, Engineering 3: 508-516 (2011).
[39] Vincheh R.M., Kargar A., Markadeh Gh.A., *A Hybrid Control Method for Maximum Power Point Tracking (MPPT) in Photovoltaic Systems*, Arabian J. Sci. Eng. 39:4715-4725 (2014).
[40] Ramaprabha R., Mathur B.L., *Intelligent Controller based Maxi-mum Power Point Tracking for Solar PV System*. Intern. J. Comp. Appl. 12(10): 37-41 (2011).
[41] Yang J, Honavar V., *Feature subset selection using a genetic algorithm*. IEEE Intelligent Systems 13 (2): 44-49 (1998).
[42] Oguz Y., Guney I., *Adaptive neuro-fuzzy inference system to improve the power quality of variable-speed wind power generation system.* Turk. J. Elec. Eng. & Comp. Sci. 18: 625-645 (2010).
[43] Arifujjaman Md., Modeling, *Simulation and Control of Grid Connected Permanent Magnet Generator (PMG)-based Small Wind Energy Conversion System.* IEEE Electrical Power & Energy Conference, Canada, pp. 1-6 (2010).
[44] Rosyadi M., Muyeen S.M., Takahashi R., Tamura J., *Transient stability enhancement of variable speed permanent magnet wind generator using adaptive pi-fuzzy controller*, Proceedings, Trondheim Power Tech. Conf., Germany, pp. 1-6 (2011).
[45] Blaabjerg F., Teodorescu R., Liserre M., Tim-bus A.V., *Overview of Control and Grid Synchronization for Distributed Power Generation Systems.* IEEE Transactions on Industrial Electronics 53: 1398-1409 (2006).

Brought to you by | Biblioteka Główna Zachodniopomorskiego Uniwersytetu Technologicznego w Szczecinie
Authenticated
Download Date | 3/5/15 11:09 AM